Supporting Information

A co-sol-emulsion-gel synthesis of tunable and uniform hollow carbon nanospheres with interconnected mesoporous

*Jianhua Hou, Tai Cao, Faryal Idrees and Chuanbao Cao,**

Reseach Centre of Materials Science, Beijing Institute of Technology, Beijing 100081, People's Republic of China.

*Corresponding Author
E-mail address: cbcao@bit.edu.cn; Tel: +86 10 6891 3792; Fax: +86 10 6891 3792.

Table S1. EDX the element composition analysis result of the core and shell for the MHSs-5-90-C/SiO_2.

Element	MHSs-5-90-C/SiO_2 (*wt.*%)			
	a	b	c	d
C	27.32	26.60	28.12	26.31
O	36.69	35.57	35.10	37.51
Si	35.99	37.83	36.78	36.18

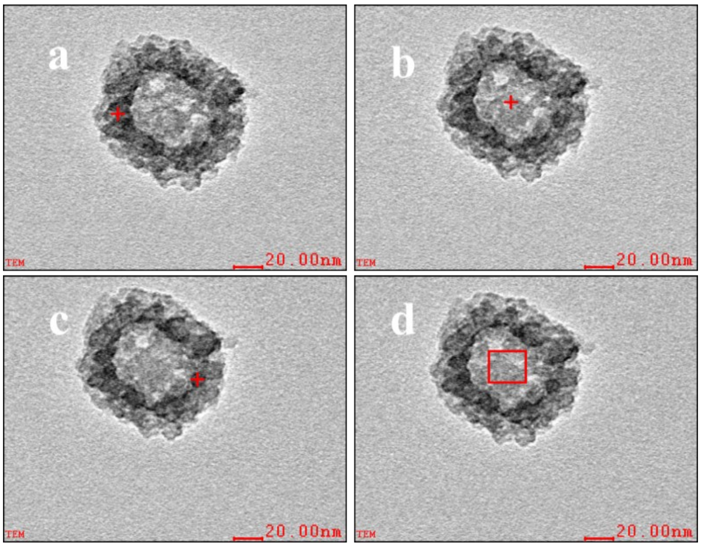

Figure S1. EDX elemental analysis of the core and shell of the MHSs-90-C/SiO_2 composites.

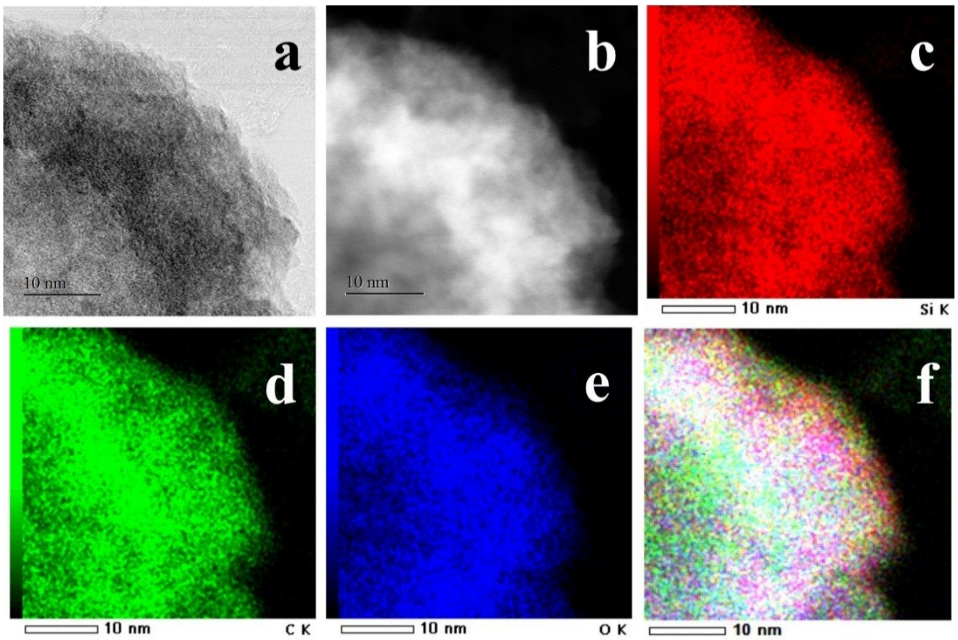

Figure S2. BF-and HAADF-STEM magnified images (a, b) of the mesoporous hollow spheres (MHSs-90-C/SiO_2), (c-e) the corresponding EDX elemental mapping of carbon, silicon, and oxygen, (f) along with an overlay of those three maps.

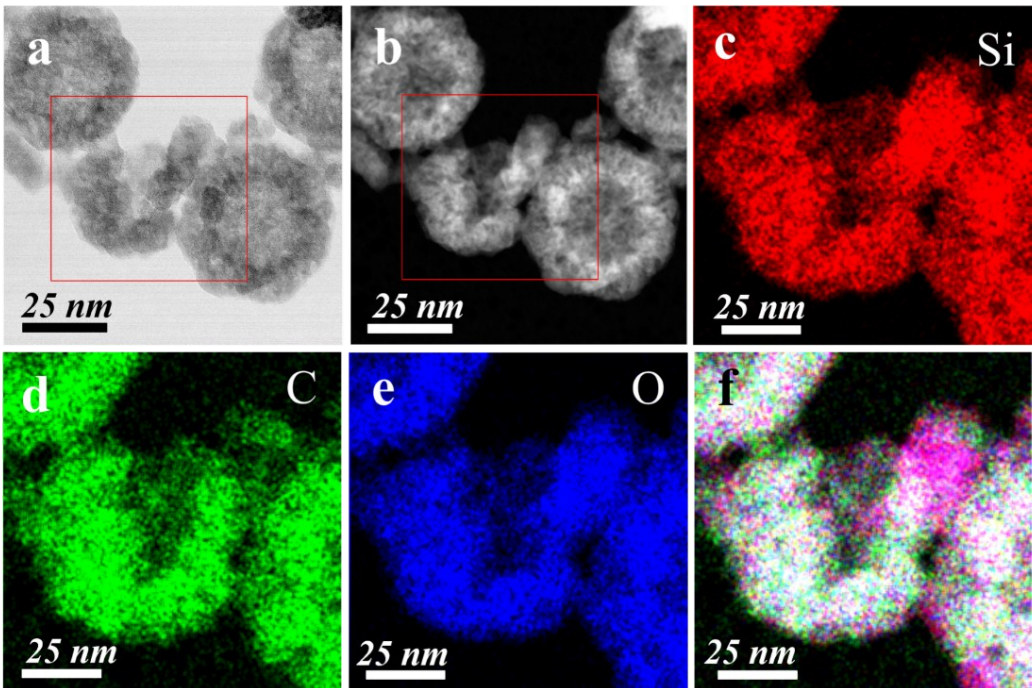

Figure S3. BF-and HAADF-STEM images of (a, b) of the wrecked mesoporous hollow sphere (MHSs-90-C/SiO_2), (c-e) the corresponding EDX elemental mapping of carbon, silicon, and oxygen, (f) along with an overlay of these three maps.

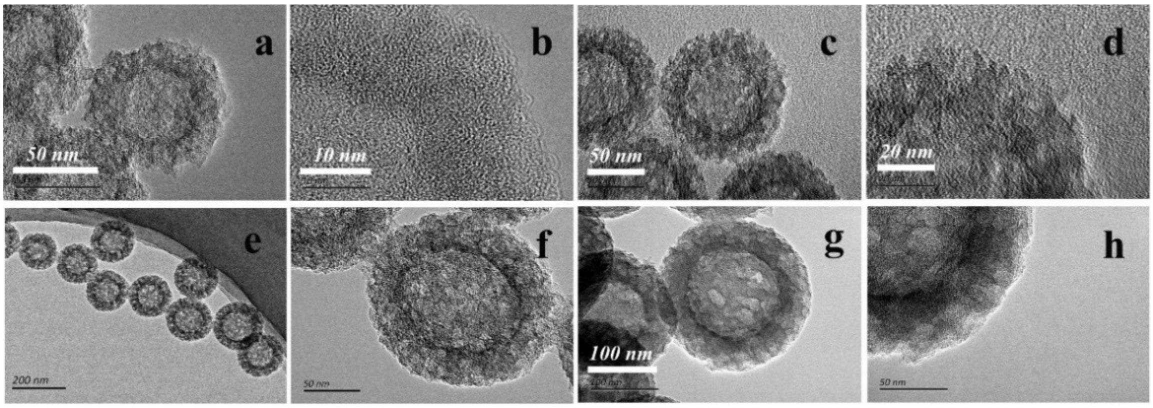

Figure S4. HRTEM images of MHCSs-90 (a, b), MHCSs-125(c, d), MHCSs-175 (e, f) and MHCSs-240 (g, h).

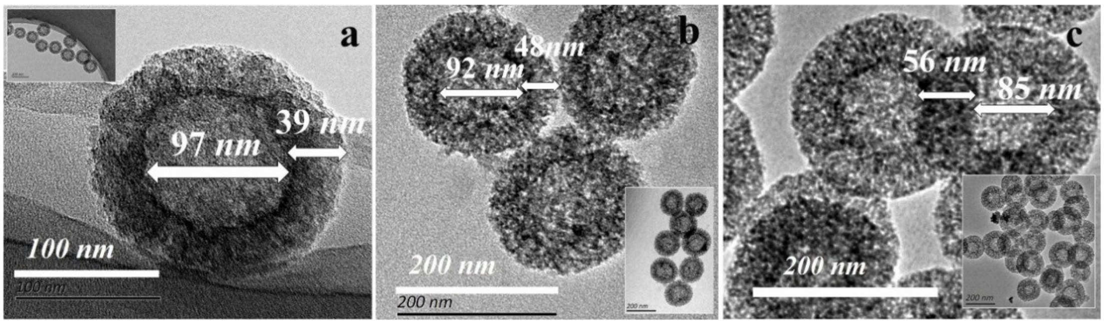

Figure S5. TEM images of (a) MHCSs-175, (TEOS-1ml); (b) MHCSs-188 (TEOS-1.5ml) and (c) MHCSs-197 (TEOS-2ml).

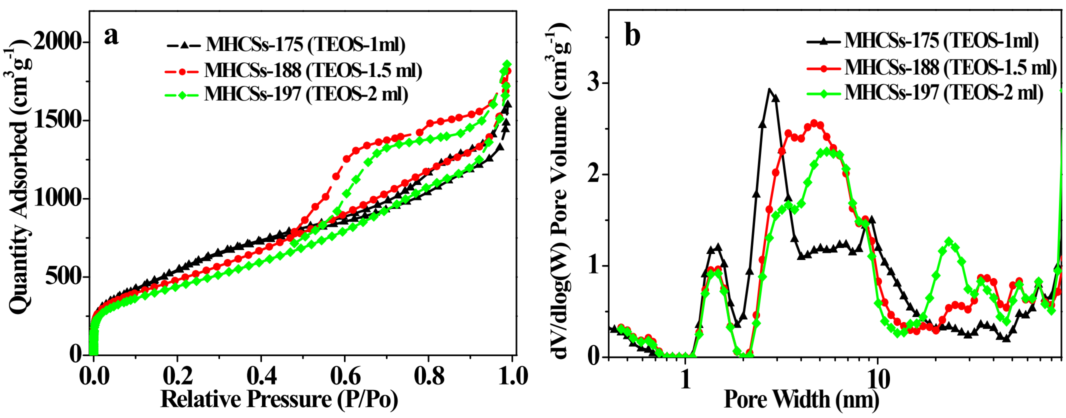

Figure S6. (a) Nitrogen adsorption-desorption isotherm; and (b) Pore size distribution of different proportions of TEOS.

Table S2. Porosity properties and distribution of pore volume of amount of different proportions of TEOS.

Sample	S_{BET}[a] (m^2/g)	Pore vol and (pore vol%) [b] (cm^3/g)			D_{aver} [c] [nm]
		V_{total}	$V_{<2\ nm}$	$V_{>2\ nm}$	
MHCSs-175(TEOS-1ml)	2203	1.96	0.25(12.8)	1. 71(78.2)	5.32
MHCSs-188 (TEOS-1.5ml)	1965	2.46	0.20(8.1)	2.26(91.9)	5.93
MHCSs-197 (TEOS-2ml)	1858	2.51	0.19(7.6)	2.32(92.4)	6.53

[a]Surface area is calculated with Brunauer–Emmett–Teller (BET) method by using a relative pressure range from 0.05-0.28. [b] The volume of pores smaller than 2 nm ($V_{<2\ nm}$), and pores larger than 2 nm ($V_{>2\ nm}$) obtained by DFT. [c] average pore diameter obtained by BET

.

Table S3. Specific surface area (S_{BET}) and pore volume of typical MHCSs and the other literature.

Samples	S_{BET} (m^2/g)	pore volume (cm^3/g)	Ref
MHCSs	2106-2225	1.95-2.53	This work
HGCS	444	0.36	5
HCS	603.8	0.32	6
OMC	1883		7
$HCMSC_{180/40}$	1314		
HCMS	1704	1.6	11
MCN	857	0.45	12
MCN_S	894-1131	1.11-1.52	13
HCSs	540 -712	0.39-0.53	17
HMCNs	646	0.38	18
HCS_S	367-466	0.6-1.6	19
HCSs	690–1370	0.49–2.33	20
HCPS	719	0.44	22
HCNPs	317.5-431.3		23
HCS	720		24
MHCSs	659- 982	1.06- 1.69	25
MHCSs	629-1321	0.66-1.05	28

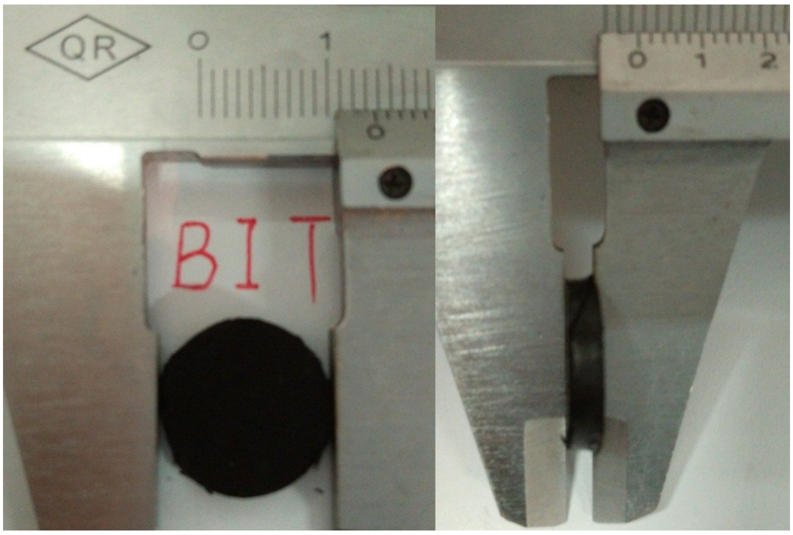

Figure S7. Radius and height of MHCSs electrode material (Formula S1 is used to calculate density of MHCSs electrode).

$$\rho = \frac{m}{v} = \frac{m}{s \bullet h} = \frac{m}{\pi r^2 \bullet h} \qquad \text{(S1)}$$

By using S1 formula density of MHCSs electrode material calculated is 0.37-0.43 g cm^{-3}, the details of it are summarized in Table S3.

Table S4. The tap density of thce electrode's material, thickness and weight of typical MHCSs

Samples	Tap density of the electrode's material (g/cm^3)	electrode's thickness (cm)	electrode's diameter (cm)	electrode's weight (mg)
MHCSs-90	0.42	0.022-0.028	1.1	8.8-11.4
MHCSs-125	0.41	0.022-0.028	1.1	8.6-11.2
MHCSs-175	0.39	0.022-0.028	1.1	8.2-10.4
MHCSs-240	0.37	0.022-0.028	1.1	7.7-9.8

Table S5. Combustion elemental analysis and XPS result of HMCSs-90

HMCSs-90	C *wt%*	N *wt%*	O wt%	F wt%	Si *wt%*	H *wt%*
XPS	94.07	1.28	3.97	0.05	0.63	-
Elemental analysis	93.43	1.21	4.64	-	-	0.72

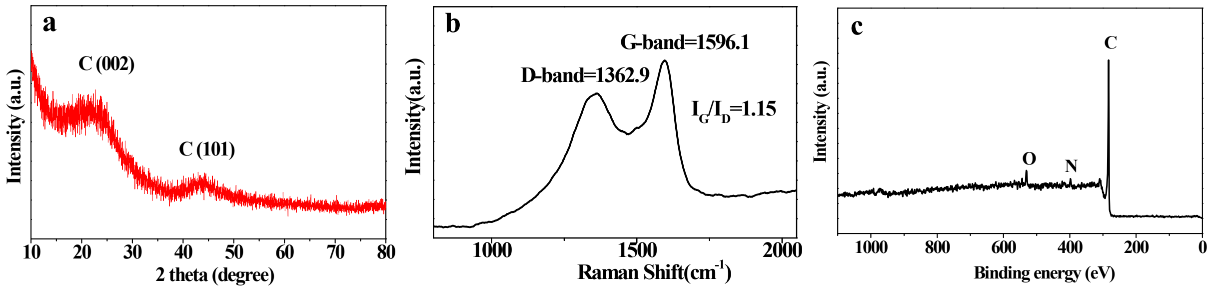

Figure S8. (a) XRD pattern, (b) Raman spectrum and (c) XPS spectra of MHCSs-90.

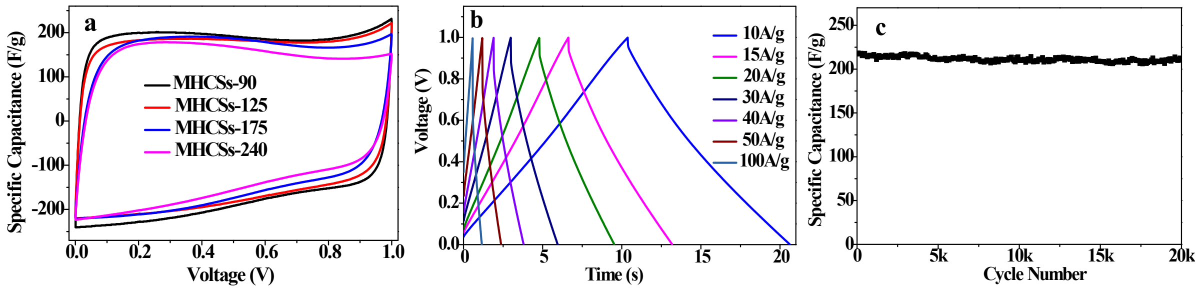

Figure S9. Electrochemical performance characteristics measured for MHCSs in a two-electrode system in 6 M KOH electrolyte. (a) Cyclic voltammograms at 0.1 V/s of MHCSs. (b) Galvanostatic charge-discharge curves of MHCSs-90 at different current densities. (c) Cycling stability of MHCSs-90 test at 5 A/g.

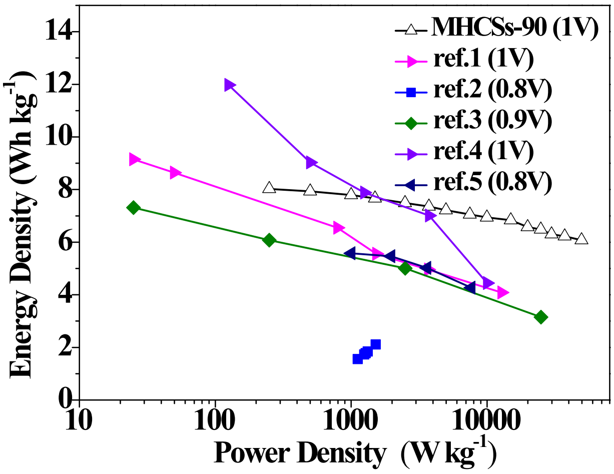

Figure S9. Ragone plot of advanced porous carbon materials that can be found in the literature with outstanding behavior as supercapacitor electrodes in H_2SO_4 or KOH electrolyte.

1 Y. S. Yun, S. Y. Cho, J. Shim, B. H. Kim, S. J. Chang, S. J. Baek, Y. S. Huh, Y. Tak, Y. W. Park, S. Park, H. J. Jin, *Adv. Mater.*, 2013, **25**, 1993-1998.

2 Z. A. Qiao, B. Guo, A. J. Binder, J. Chen, G. M. Veith, S. Dai, *Nano Lett.*, 2013, **13**, 207-212.

3 K. Xie, X. Qin, X. Wang, Y. Wang, H. Tao, Q. Wu, L. Yang, Z.Hu, *Adv. Mater.*, 2012, **24**, 347-352.

4 W. Qian, F. Sun, Y. Xu, L. Qiu, C. Liu, S. Wang, F. Yan, *Energy Environ. Sci.,* 2014, **7**, 379-386.

5 B. You, J. Yang, Y. Sun, Q. Su, *Chem. Commun.*, 2011, **47**,12364-12366.